Lessons Learned in Fabrication of a High-Specific-Torque Concentric Magnetic Gear

Zachary A. Cameron
Research Aerospace Engineer
NASA Glenn Research Center
Cleveland, OH, USA

Thomas T. Tallerico
Research Aerospace Engineer
NASA Glenn Research Center
Cleveland, OH, USA

Justin J. Scheidler
Research Aerospace Engineer
NASA Glenn Research Center
Cleveland, OH, USA

ABSTRACT

Magnetic gearing is being investigated at NASA as a replacement to conventional mechanical gearing in aerospace applications. Some potential benefits of magnetic gears over mechanical gearing are torque transmission without mechanical contact, decreased transmission noise, and no required lubrication. However, in order to be a viable alternative for aerospace applications, magnetic gearing must be shown to provide high enough specific torque (torque per unit mass). NASA's second magnetic gearing prototype (PT-2) was able to achieve promising specific torque on par with low torque mechanical gearboxes. This work will briefly review the electromagnetic and structural design of PT-2, provide detailed information on fabrication and assembly, examine build errors, walk through rebuild efforts to improve operation, and conclude with remarks on build difficulties and opportunities for improvement in future prototypes.

INTRODUCTION

Concentric magnetic gears (CMGs) provide a gear ratio by magnetically coupling two magnetic arrays of different pole counts via a magnetic flux modulating body made from soft magnetic materials. An example of a CMG's cross-section is shown in Figure 1. A CMG can be viewed as analogous to planetary gears with, the sun and ring magnetic arrays (referred to as sun and ring gears throughout this work) comparable to mechanical sun and ring gears, and the modulator acting as the planet gears. CMG's, when compared to many other magnetic gear designs, keep the majority of their magnets simultaneously engaged in torque transmission. Because of this, they show greater potential for higher specific torque, leading to CMGs being the main focus of magnetic gearing research at NASA for use in aerospace applications.

One application under investigation for CMGs is in the propulsors of urban air mobility (UAM) vehicles (Refs. 1, 2), which are intended for short range point-to-point, origin-to-destination air travel. UAM is looking to make use of electrified vertical takeoff and landing (eVTOL) aircraft designs due to the limited runway space available in crowded urban environments. Operation in crowded urban environments also demands reduced noise emissions from UAM aircraft. To achieve this, many UAM eVTOL designs reduce aircraft noise, and in turn improve aerodynamic performance, through the use of smaller distributed rotors driven by electric motors (Ref. 3). Pairing electric motors with gearboxes reduces the torque required to be produced by an electric motor. This provides significant volume, weight and in many cases efficiency gains over direct drive solutions (Ref. 4). This is due to the fact that an electric motor's volume and mass decrease as output torque decreases (Refs. 3, 5, 6). Mechanical gearboxes, however, are prone to failure in rotor-craft systems (Refs. 7–9). Therefore, while adding a gearbox to an eVTOL propulsion system can provide weight and efficiency benefits, it comes at the cost of possibly lower reliability. Lowering eVTOl aircraft reliability would increase down time and repair costs of a fleet with high expected utilization (exceeding 2,000 flight hours per year) and demanding low operating costs (Ref. 10). In contrast to conventional gearing, magnetic gears provide transmission of torque via non-contacting components, which has potential to increase reliability and reduce maintenance. While magnetic gearing's possible reduced maintenance is attractive, in order to be viable in eVTOL applications or other aerospace systems, the specific torque and efficiency of CMG's must be competitive with conventional gearing.

NASA has therefore laid out a road map to achieve high performance CMGs in three phases. The first phase of work, reported on in (Ref. 1), focused on development of a core understanding of magnetic gearing technology and fabrication of a prototype (PT-1) to display CMG working principles. This work was expanded upon and used to produce a second magnetic gear prototype (PT-2) which is the focus of this work. Phase two, which is currently coming to a close, was focused on the realization of a high specific torque and high efficiency CMG design (PT-3). Phase three will focus on the integration of magnetic gears with electric motors to provide a high efficiency, reliable, and low mass electric drive

Presented at the Vertical Flight Society 75th Annual Forum & Technology Display, Philadelphia, Pennsylvania, May 13–16, 2019.

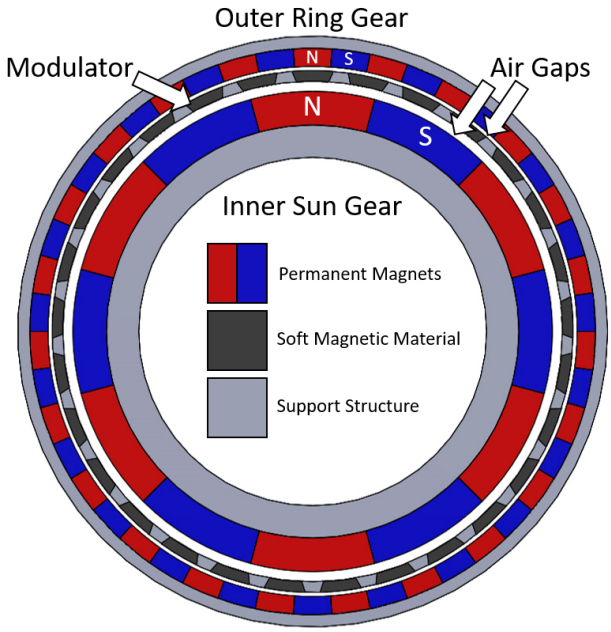

Fig. 1. Concentric magnetic gear cutaway view showing air gaps separating the three primary components; inner magnetic "sun gear", outer magnetic "ring gear", and soft magnetic material modulator.

system for aerospace applications. Each prototype is intended to be a technology demonstrator, provide test data to validate magnetic finite element analyses (FEA), and act as a learning tool with regards to high performance CMG fabrication. This paper's goal is to review the fabrication and assembly of PT-2. In doing so, it will highlight key challenges when fabricating components in high specific torque CMGs and provide detailed explanations of methods used.

PROTOTYPE 2 DEVELOPMENT

PT-2 was designed to be a high specific torque version of NASA's first magnetic gear prototype PT-1. PT-1 was designed as a proof of concept magnetic gear for NASA's Maxwell X-57 high lift propulsors. It used off the shelf magnets, and had a specific torque of 20 Nm/kg (6.7 ft lbf/lb). Its input shaft was connected to the sun gear and its output shaft connected to the modulator, with the ring gear held stationary. The same configuration of rotating and stationary components was used for PT-2, along with a similar outer diameter of approximately 140 mm (5.5 in). PT-2 also had a designed output speed of 4000 RPM, and gear ratio of 4.83:1, similar to PT-1. A major difference between PT-1 and PT-2 was axial magnetic active length was doubled to 50.8 mm (2 in) for PT-2. This improved PT-2's aspect ratio (length to diameter ratio) which reduced undesirable 3D magnetic leakage effects (Ref. 11). The magnetic circuit was then re-optimized as discussed in (Ref. 1). The resulting dimensions of the gear's magnetic circuit are presented in Table 1. Once completed, measured specific torque of PT-2 was approximately 45 Nm/kg (15 ft lbf/lb).

Table 1. Prototype-2 magnetic array design parameters when optimized for specific torque using N52 magnets and HF-10 in modulator

Characteristic	Metric	English
Gear Ratio	4.83:1	
Sun Pole Pairs	6	
Ring Pole Pairs	23	
Modulator Poles	29	
Magnets Per Sun Pole Pair	6	
Magnets Per Ring Pole Pair	6	
Outer Diameter	140.5 mm	5.531 in
Sun Magnet Thickness	8.35 mm	0.329 in
Ring Magnet Thickness	4.55 mm	0.179 in
Modulator Thickness	2.65 mm	0.104 in
Modulator Outer Span Angle	9.17 deg	
Modulator Inner Span Angle	7.45 deg	
Sun-Modulator Air Gap	2.5 mm	0.098 in
Ring-Modulator Air Gap	1.0 mm	0.039 in
Axial Length	50.8 mm	2 in
Maximum Output Torque	127 N-m	94 ft-lbs
Magnetic Array Mass	2.9 kg	6.4 lbs
Modulator Lamination Thickness	0.254 mm	0.010 in

There were three major changes made in PT-2 relative to PT-1 to improve specific torque that lead to significant structural and fabrication challenges. The first was the use of six-magnet Halbach arrays with custom magnets on both the sun and ring gears. Second was a reduction in modulator radial thickness, down to 2.65 mm (0.104 in). The third change was removal of non-magnetic structural walls from the outer and inner diameter of the modulator and inner diameter of the ring gear. This was done to reduce air gap sizes and improve performance. The structural and fabrication challenges associated with each of these changes will be discussed in depth below.

The use of Halbach arrays has been found to improve the performance of magnetic gears (Refs. 12,13). In parametric studies of Halbach arrays discussed in (Ref. 1), it was found that increasing the number of magnets per pole pair from four to six in a Halbach array improved specific flux (flux per magnetic array mass). Going beyond six magnets per pole pair offered little additional specific flux improvements at a significant increase in cost and complexity. Therefore six magnet Halbach arrays were used in PT-2 for both the ring and sun gears. An example of a six magnet array is depicted in Figure 2 with directional nomenclature associated with magnetization included (North-N, South-S, East-E, and West-W). Halbach arrays in PT-2 were constructed from custom arc segment magnets as depicted in Figure 3 in order to obtain high magnetic fill percentage in the sun and ring gears. The use of custom arc segments increased the manufacturing complexity by requiring thinner support and alignment structures between magnets. It also increased tolerance requirements for the additively manufactured parts to ensure proper assembly.

During the design of PT-2, it was found that one of the major drivers of a magnetic gear's specific torque is modulator thickness. (Ref. 14) shows that torque per magnet mass always de-

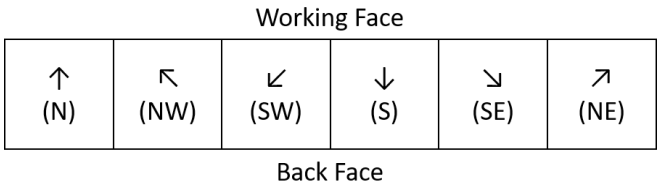

Fig. 2. Single pole pair of a six magnet Halbach array configuration showing magnetization direction via arrows and direction nomenclature for reference.

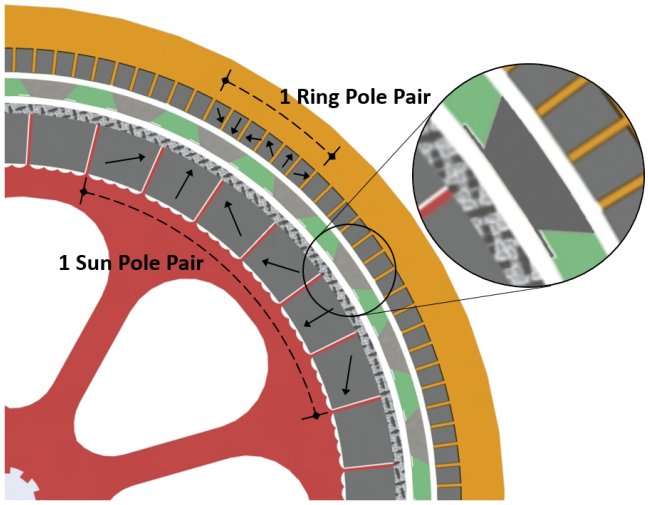

Fig. 3. PT-2 magnetic arrays displaying sun and ring pole pair magnetization directions and modulator cross-section in expanded view.

cays with magnet thickness while overall torque increases. To optimize electromagnetic specific torque of a CMG for a set outer radius and torque, however, there is an optimum magnet thickness value. This optimum magnet thickness is driven by the modulator's thickness and air gap thicknesses. For a fixed set of air gap thicknesses, the optimal modulator thickness will be as thin as possible without diminishment of the modulation effect. A thinner modulator then leads to thinner magnets when optimizing for specific torque. This is because there is less modulator mass that the magnet array's flux has to produce torque to compensate for. Therefore, reduced modulator thickness both reduces modulator mass and magnet mass at a given torque. Unfortunately, the electromagnetically optimum modulator thickness is typically thinner than what is mechanically viable at output torques investigated in this work. For PT-2, a modulator thickness of 2.65 mm (0.104 in) was found to be near optimal electromagnetically and provided sufficient space for structural material. Although, it also meant there was little margin for alignment error during modulator assembly. It also meant that support structure and pole piece stiffness was a critical aspect of PT-2's design.

Finally, as also discussed in (Ref. 1), a magnetic gear's specific torque is heavily influenced by the size of the magnetic air gap between the ring gear and modulator. The short pole to pole distances on a CMG's ring gear makes the magnetic reluctance (resistance to storing magnetic energy) through the outer air gap low. If the reluctance through the air gap is lower than the reluctance of the coupling path to the modulator and sun gear, then a significant portion of the ring gear's flux will not produce torque. Increasing ring-modulator air gap size increases the reluctance of the coupling path. Therefore, minimizing the size of the ring-modulator air gap is important for maximizing coupling, significantly improving a magnetic gear's specific torque. To that end, PT-2 was designed without structural walls that existed in the ring-modulator air gap of PT-1. The elimination of these structural walls led to significant structural design and assembly challenges. Retaining "feet" had to be added to the pole pieces, as depicted in the cutout view in Figure 3. This restrained pole pieces mechanically in the radial outward direction while minimizing impact on specific torque. The ring magnets, without an inner wall, had to be surface mounted, which meant strong adhesives were necessary to hold them in place.

In the following sections, the issues encountered in the design and fabrication of PT-2 associated with the three, aforementioned, major design decisions will be discussed in detail. Challenges and points of required improvements will be discussed. Other structural aspects such as the sun gear's rotor-spoke configuration, carbon fiber retaining hoop thickness, the ring gear's outer wall thicknesses, cap thicknesses, shaft diameters, spline geometries, and the size of bearings were selected through iterative design development stages. These choices were made with basic governing physics equations and validated through the use of FEA with the goal of minimum system weight. Additively manufactured continuous-strand-carbon-fiber-reinforced nylon was used for the majority of the structural components. This was due to its lack of magnetic interference, reasonable strength, speedy manufacturing, quick availability, relatively low cost, and light weight.

Sun and Ring Gear Fabrication

The sun gear's assembly was performed in one step, where all of the magnets were populated, with adhesive, in a single session and allowed to cure. The carbon fiber hoop that structurally contained the magnets was installed on the rotor before populating the magnetic array to prevent the magnets from becoming radially misaligned. Additionally, a set of acrylic rings were fit around the outer diameter of the carbon fiber hoop to provide support and prevent any deflection. The sun rotor, carbon fiber hoop, and a single acrylic ring along with a test fit magnet can be seen in Figure 4.

The sun gear's Halbach array assembly order was chosen such that the magnetic forces resisting assembly were minimal. For the first half of a Halbach array pole pair, the southwest and southeast magnets were slid into their respective slots with adhesive, followed by a south magnet in between the two. This half of the pole pair was then checked with a piece of magnet viewing paper to verify that magnetic alignment was correct. Then, the second half of the pole pair was assembled. A northeast and northwest magnet were slid into place with adhesive

Fig. 4. Sun rotor with carbon fiber hoop bound by acrylic ring; single magnet test fit into slot.

Working Face

↙ (1)	↓ (3)	↘ (2)	↗ (4)	↑ (6)	↖ (5)

Back Face

Fig. 5. Halbach array magnet assembly order where all of the magnets' adhesive cured simultaneously.

followed by a north magnet in between. Once again, the magnetic alignment was checked with viewing paper. This assembly order is displayed in Figure 5 . From here, the process was continued in a circular pattern about the sun rotor for the remaining pole pairs. Once the adhesive fully cured the acrylic retaining rings were removed, and the high speed aluminum input shaft was then pressed into the sun's rotor splines. The appropriate bearings were then pressed onto the high speed shaft. This sub-assembly, which can be seen in Figure 6, was then set aside.

The ring gear's fabrication process was similar to the approach used for the sun gear. The order of magnet population depicted in Figure 5 was used again. One notable change was that there was no carbon fiber hoop to constrain the magnets in the ring. Instead a thin wall on the inner diameter of the ring structure, made from the same material as the bulk structure, was included. This thin wall was intended to be removed after magnets were in place and the adhesive cured fully. An additional change was the inclusion of locating posts in the assembly process. Due to how thin the ring gear's magnets were, they were very difficult to handle. To make handling simpler, slots that the magnets were to be placed in to were over-sized radially. This made sliding individual magnets into their respective slots, while being attracted through magnetic forces to their neighbor, more manageable. A carbon fiber reinforced nylon post was pressed into the radially outward side

Fig. 6. PT-2 sun rotor sub-assembly including fully cured magnetic array, carbon fiber retaining hoop, high speed shaft, and bearing.

of the slot along with each magnet. This forced the magnets inward to their appropriate radial location. This manufacturing process can be seen in Figure 7.

Once the adhesives bonding the magnets to the rotor were fully cured, the interior wall was carefully removed. Due to the eventual placement of a cap on the top of the ring gear, the portions of the locating posts extending axially beyond the magnets had to be removed as well. The final ring gear magnetic array can be seen in Figure 8.

Modulator Fabrication

The fabrication of the modulator was by far the most challenging aspect of manufacturing PT-2, and it appears to be a prevalent manufacturing challenge for CMGs in general. Previous prototype builds in (Refs. 15–17) had individual modulator segments connected with bridges, making a single body of soft magnetic material that they reinforced with non magnetic material. This method, while somewhat simpler in manufacturing, comes at the cost of decreased torque capacity. This reduction is due to the bridges altering the reluctance paths between the sun and ring gear, causing decreased coupling. In addition to bridges connecting pole pieces, many designs commonly found in the literature have modulators that are thicker radially, providing greater structural stiffness. Despite what was found in literature, the final design selected for PT-2 did not include connecting rings and was also as thin radially as determined mechanically allowable. While these selections enabled higher specific torque, they also added structural complexity to the modulator's body.

The first complexity to tackle was fabrication of the modulator pieces themselves. Without a ring connecting all the indi-

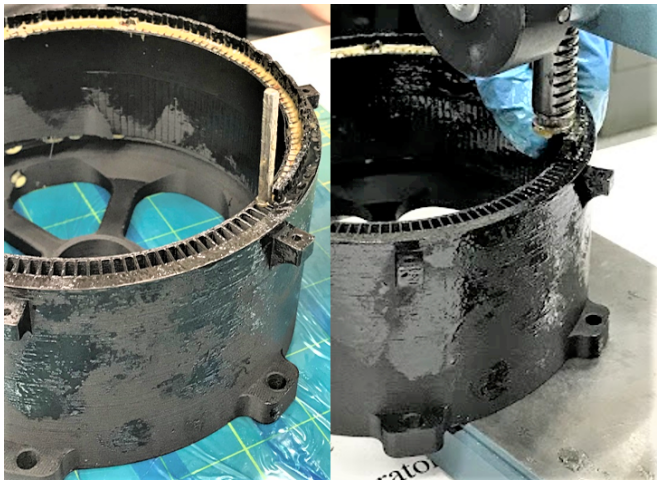

Fig. 7. PT-2 ring gear mid-assembly process showing magnet located in slot without locating post on the left and being pressed into location with locating post on the right.

vidual pole pieces, they had to be manufactured individually. PT-1's pole pieces had no connecting ring either, and had been manufactured by laser cutting pole piece cross-sections from thin silicon steel lamina. These lamina were then stacked and bonded to length. Due to the manufacturing complexity and high cost associated with this method for the smaller and more delicate cross-sections of PT-2, this method was not an option. Instead, it was decided to have a large 25.4 mm (1 in) thick plate of stacked and bonded lamina fabricated. The plate thickness was selected based upon bonding adhesive limitations when dealing with large cross-sections. From this plate, individual pole pieces were cut via wire EDM and stacked to create the desired overall 50.8 mm (2 in) thickness. While the wire EDM was able to accurately cut the small delicate cross-sections, the individual lamina separated from one another as shown in Figure 9. The cause of this separation is unclear. One possibility, is it occurred due to the exposure of the laminated plates to the dielectric fluid required for cutting. Another possibility is that localized heating from the wire cutting through the thin cross-sections warmed the adhesive between lamina beyond its glass temperature. Despite their fragility and the high number of pieces they had broken in to, it was decided to use the pieces anyway. Individual poles pieces for PT-2 were assembled from the small segments and glued together to make a piece as close as possible to the desired length.

For PT-2, additively manufactured carbon fiber reinforced nylon parts were the most reasonable choice for structures. Careful selection of fiber direction was critical to provide the stiffness required. For the modulator, due to its hollow cylindrical shape and the thin radial air gaps between it and the magnetic arrays, achieving minimum radial deflection was critical. To achieve this, the caps on the top and bottom of the modulator were manufactured with concentric rings of continuous carbon fiber to provide maximum hoop stiffness. Reinforcing posts that pressed into the caps, and lay between the pole pieces, contained fibers running lengthwise (axially).

Fig. 8. PT-2 ring gear sub-assembly with fabrication features removed and ready for assembly.

While there was mechanical interlocking between the poles and posts, stiffness was also provided by adhesion of the pieces with high strength epoxy.

Modulator assembly began with the thicker of the two caps, referred to as the bottom cap. Support posts were placed in slots around the circumference of the cap and a press fit held them in place. An outer mold was then placed around the cap and posts to maintain the desired circumference when pole pieces were added. Pole pieces were then slid in between the structural posts with the interlocking faces covered with adhesive. Due to the previously mentioned process of stacking dislocated pole pieces to the appropriate length, some stacks were slightly larger and some slightly smaller when in the assembly. Once fully populated with structural posts and poles, the part was allowed to rest and adhesive cure fully. The mold was then removed and the output shaft with its bearing already in place was slid into the modulator. Retaining bolts were then screwed into place and the sub-assembly was ready for assembly with the other components.

Magnetic Gear Assembly

To complete assembly, the three concentric bodies of the magnetic gear needed to be carefully nested inside one another. Once fully assembled, appropriately seated bearings maintain the bodies concentrically. Until then, the magnetic forces tended to pull the components out of concentricity and into contact with one another. In order to resist these forces, reduce incidental contact of magnetic bodies, and ensure concentricity in assembly, a lathe and shims were used for assembly.

The first bodies needing to be assembled were the sun gear and modulator. The sun gear was slid into the modulator on a lathe through use of a temporary guide shaft. The guide shaft

Fig. 9. Electrical steel lamina separated from one another after wire EDM process with 1 in (25.4 mm) section laid out in a row on the right.

had a threaded tip that screwed into the end of the input shaft that was pressed into the sun gear. Once in the lathe, the guide shaft's outer diameter slid into the inner diameter of the output shaft on the modulator, and could be used as a locator to feed the sun body into the modulator. This maintained component's concentricity and is shown in Figure 10. A cap was then pressed on to the other end of the modulator to fully contain the sun gear and support the sun gear's bearing. The final sun-modulator sub-assembly, with all hardware installed, can be seen in Figure 11.

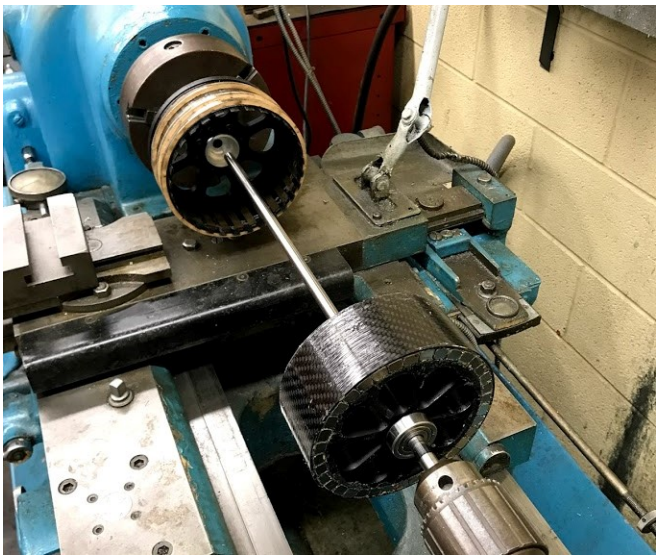

Fig. 10. PT-2 sun gear (right) guided into the modulator (left) with temporary guide shaft screwed on to maintain concentricity in assembly.

For the final assembly step, the ring gear was then fixed to a bench top for the insertion of the sun-modulator sub-assembly. This was due to the ring being too large to fit on the lathe. Guide ways were temporarily attached to the ring gear to guide the sun-modulator sub-assembly in. Shims were

Fig. 11. PT-2 sun gear and modulator subassembly ready for assembly with ring gear, with dark lines on modulator pole pieces showing where separations occurred in wire EDM cutting process.

also included on the inside diameter of the ring gear to maintain the desired air gaps until the bearing was rightfully seated in the output shaft's bearing cup. Both of these features can be seen in Figure 12. The sun-modulator sub-assembly was then gently lowered via crane into the ring gear. The crane allowed for the sun-modulator sub-assembly's descent to be carefully controlled. Once the sun-modulator sub-assembly was fully inside the ring gear, and the bearing was confirmed to be properly seated, the final cap was secured to the top of the ring gear. This locked all of the components in place concentrically and the shims could then be removed from the air gap. The fully assembled gear is depicted in Figure 13.

Once final assembly was completed, static pullout torque testing was performed and the gear ratio was confirmed to be correct. Some rubbing could be felt and heard between components, but due to how tightly nested the structures were it was very difficult to determine where contact was occurring. The following sections discuss the determination of what components were rubbing and the attempts to fix this issue are explored.

PROTOTYPE-2 ISSUES AND REBUILDS

Although the final gear assembly was capable of transmitting torque and was confirmed to have the appropriate gear ratio, components were contacting one another and resisting rotation. In order to determine which components were rubbing, the gear needed to be disassembled. Once disassembled, a marking compound was applied to the modulator so that when the gear was reassembled and rotated, the compound would reveal where contact was occurring. After reassembly, rotation, and dis-assembly, wear in the marking compound revealed significant contact between the modulator and the ring

Fig. 12. Ring gear bolted to a bench-top with six guide-ways attached to its top ready for assembly with sun-modulator sub-assembly.

Fig. 13. PT-2 fully assembled with the axial face of the sun gear magnets visible through the modulator and ring gear caps.

gear, but no evidence of contact between the sun gear and modulator. The rubbing observed can be seen in Figures 14 and 15.

There are multiple sources of error which together led to the ring gear and modulator bodies contacting. The first is errors in the manufacturing process of the Halbach arrays for the ring and sun gears that led some magnets to be out of place radially. The second source of error is due to a lack of stiffness in the modulator from pole pieces, support posts, and the final cap. These sources of errors will be further discussed below and efforts to correct for these errors will be laid out.

Halbach Array Manufacturing Errors

With the knowledge that the modulator and ring magnets were rubbing, the sun and ring magnetic arrays were inspected more carefully. The magnets on the ring gear that were contacting the modulator were found to be the north and south magnetized magnets in the Halbach array. They were raised above the other magnets in the Halbach array, some by as much as 0.25 mm (0.01 in). This is logical, due to magnetic forces within the Halbach array having a tendency to apply force to the north and south magnets in the direction of the working face (outward radially on the sun gear and inward on the ring gear). Upon further inspection of the sun gear, it was also found to have slightly bulging north and south magnets in its Halbach array despite containment via its carbon fiber hoop.

The misalignment of the north and south magnets in both magnetic arrays is attributed to two faults. The first being that the carbon fiber hoop on the sun and the retaining wall on the ring were not sufficiently stiff enough to hold the magnets in place while the adhesive cured. The second being that the entire Halbach array was populated simultaneously, so that the individual magnets would be subject to forces from their neighbors in the array while curing. In an attempt to correct these errors, an additional test trial using an alternative fabrication method was performed. In this test trial, spare magnets were assembled in a six magnet Halbach array on a sun rotor section. The array was assembled two magnets at a time (north and south, northwest and southeast, or southwest and northeast) across the entire sun rotor section. The epoxy was allowed to cure fully between assembly of each set. The exact order that was used can be seen in Figure 16. Over-sized molds were made to provide ample stiffness and to prevent movement of magnets while the epoxy cured. These molds were specialized for each of the three steps, the latter two of which required an additional mold cap. The mold cap provided an extended channel that aligned and supported the magnets while they were pushed into place with a small plunger. The plunger was necessary to overcome the magnetic forces. Once the magnet was in place, the cap and plunger could then be clamped down while the epoxy cured. Before use, a release agent was applied to all the molds, plungers, and caps so that the adhesive would not bond with them and the molds would be easier to remove. The test trials yielded positive results with all magnets retained in their appropriate locations, proving the efficacy of the method.

Due to budget and time constraints, the improved method de-

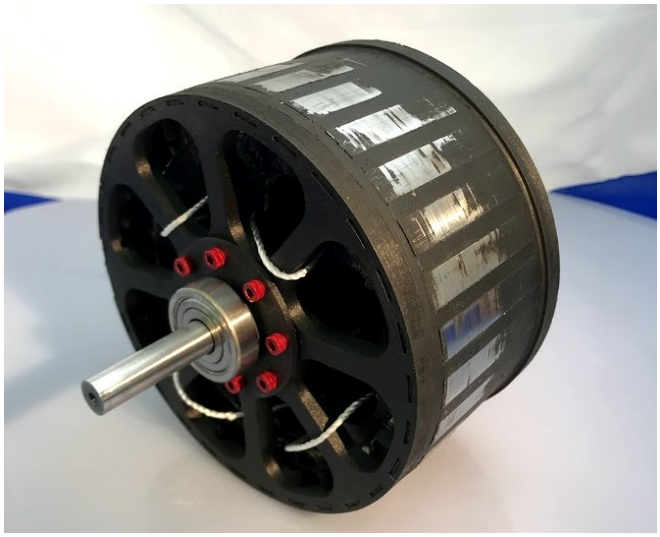

Fig. 14. Modulator after contact had occurred showing marking compound removed towards the end of the modulator where its final cap was applied.

Fig. 15. Ring gear after contact had occurred showing marking compound on every third magnet examples of which are circled in red.

scribed above could not be utilized to rebuild the PT-2 sun and ring gear magnetic arrays. The magnets from the arrays could not be reused due to the high risk of magnet damage when attempting to remove them from the arrays. Instead, the method was documented and planned for use in the fabrication of PT-3.

Difficulties With Modulator Stiffness

Modulator stiffness was the second error source that led to components contacting in operation of PT-2. Based upon careful examination, it was determined that the modulator must be deflecting excessively when magnetic forces were applied to it due to insufficient stiffness. This conclusion was based on the fact that almost exclusively the center span of the modulator pole pieces was making contact with the ring gear. Upon measurement, it was found that the magnets on the ring gear were protruding evenly across the entire axial length. If the ring gear magnets' misalignment was the sole cause of the contact, then the entire length of the modulator would show contact. It was also observed that the contacted region on the modulator was slightly shifted towards the end

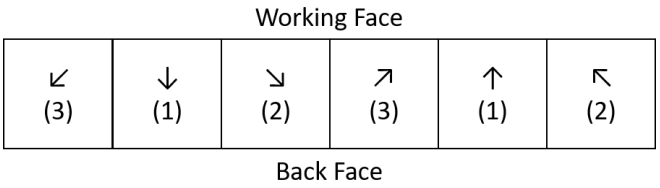

Fig. 16. Refined Halbach array magnet assembly order where north and south, southeast and north west, and southwest and northeast magnets were bonded in separate steps.

of the modulator with the thinner cap. This can be observed in Figure 14 where the thinner cap is towards the camera. Along with this evidence, updated FEA was performed that assumed no stiffness from the modulator's steel pole pieces. This assumption seemed reasonable due to the fact that the lamina's bonding failed when cut with wire EDM as shown in Figure 9. The updated results showed deflections greater than expected, with peak deflections in the region where the most rubbing was observed.

In light of all of this, multiple sources were cited as contributing to a lack of required stiffness. The first, being the radially smaller cap that finished the modulator assembly lacking sufficient stiffness. The second was a failure of the laminated pole piece bonding agent during the wire EDM process, which meant that they provided essentially no stiffness to the subassembly. The third was that the structural posts were not stiff enough on their own to prevent excessive deflection. These three issues are addressed in the following section with a rebuild of the PT-2 modulator.

Modulator Rebuild

In order to make use of the existing magnetic arrays, it was determined the most feasible endeavor that provided the most value to the project was to develop a second, stiffer modulator. In order to make the modulator stiffer, three major design changes were made: the end cap of the modulator was stiffened, the cross-section of the steel pole pieces was altered, and an alternative method of pole piece manufacturing was used.

The first major change was the stiffening of the second cap on the modulator. The cap was redesigned to have the maximum diameter possible while still fitting through the ring gear's magnetic array during the assembly process. This slight diameter increase provided additional space for continuous carbon fiber strands increasing cap stiffness.

The second change was in the design of the steel pole pieces. The pole piece's structural feet were expanded and rounded while maintaining the same inner and outer diameter and span angles as seen in Figure 17. This made the faces that interlocked with the structural posts a smoothed curve instead of a sharp flat, thereby increasing contact area. This design also reduced stress concentrations in the feet of the pole pieces and improved stiffness.

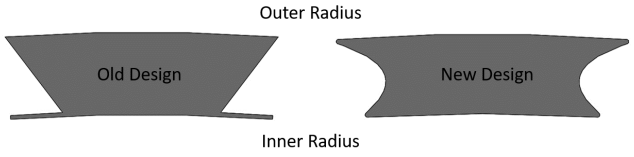

Fig. 17. Modulator pole piece cross-section redesigned to improve manufacturability and the retaining foot's structural strength and stiffness.

The third change was in the fabrication method of the pole pieces. In an attempt to avoid the failure of lamina bonding in the pole pieces, the wire EDM process was completely eliminated. Instead of cutting all of the pole pieces from a single pre-stacked and bonded block of lamina, each layer of all the pole pieces was laser cut out of a single 0.254 mm (0.01 in) sheet. An exterior ring 1 mm (0.04 in) thick held all of the cross-sections together in their final positions. These cutouts were then staked and bonded to the full 50.8 mm (2 in) height desired. The ring-bound pole pieces were then placed on the first modulator cap, and the support posts were coated in adhesive and then pressed into place. After the adhesive cured, the ring connecting the pieces together was machined off carefully. This process also ensured that all the pole pieces were the same diameter. The outer surface was then lightly sanded with high grit sand paper to ensure there was no electrical shorting between the lamina. A final light layer of epoxy coating was applied to the surface to prevent any oxidation. The rebuilt modulator for PT-2 can be seen in Figure 18 along with the improved cap laying next to it. A major benefit of this method, unlike the previous method, was that the pole pieces were intact and fully bonded in the assembly. In addition to this, all poles were also of equal length and their outer diameter correct.

The new modulator was then ready for reassembly with the sun and ring gears. The same assembly method as before was used to put together the sun and modulator. This sub-assembly was then lowered into the ring gear via crane, but shims were no longer necessary due to the larger cap contacting the inner diameter of the ring gear and acting as a guide until the bearings were properly seated. With this new assembly, contact between the three bodies was eliminated. New pullout torque measurements were taken, and the prototype was then installed in a test rig for dynamic testing.

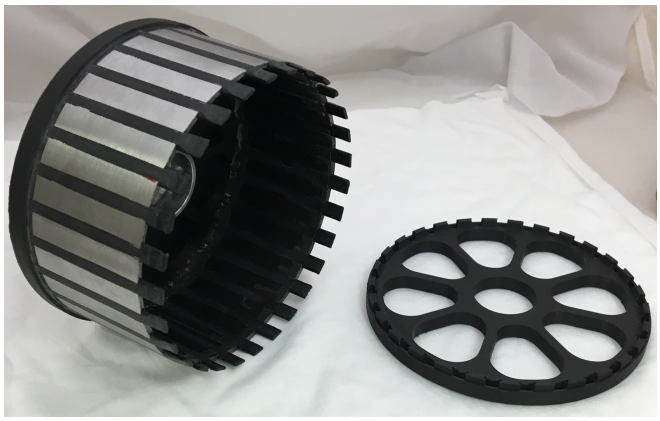

Fig. 18. Improved modulator design after bounding hoop was machined off with stiffer end cap seen to the right.

Testing and Failure

Work by Scheidler et al. in (Ref. 2) lays out the testing capabilities of the E-Drives Rig developed at NASA for the testing of magnetic gears and small scale electric motors. An additional paper titled "Dynamic Testing of a High-Specific-Torque Concentric Magnetic Gear" by the same author will provide dynamic testing results of the PT-2 magnetic gear on the E-Drives Rig for readers interested in a more in depth look at test specifications and the gear's performance. In this work, only failure of the gear after testing is discussed.

After some tests were performed in the E-Drives Rig, an irregular noise developed. Testing was halted and PT-2 was partially disassembled. Upon disassembly, it was found that one of the modulator's pole pieces had broken. It appears that some of the lamina within one of the pole pieces had dislocated from one another. Either mechanical action, magnetic action, or a combination of the two appear to have worked the dislocated lamina back and forth against the pole piece's neighboring support posts. This action effectively dug into and removed some of the support material. The resulting damage can be seen in Figure 19.

Fig. 19. PT-2 second modulator with sun gear still inside after testing resulted in a broken pole piece.

PT-2 was then fully disassembled and the modulator was mended to the best of the team's ability. At the time of testing PT-2, the fabrication of PT-3 was underway, which utilized a

slightly different modulator fabrication method. PT-3's fabrication method yielded surplus modulator poles that had the same geometry as the PT-2 poles. One of the surplus poles was used to replace the destroyed pole in the PT-2 modulator. Unfortunately, due to adhesive applied to the ends of the support posts, the damaged posts could not be removed and replaced due to fears of damaging additional poles. Instead, the replacement modulator pole and existing damaged support posts were fixed in place with molds and the voids filled with a high strength epoxy resin. Once fully cured, the modulator was reassembled with the sun and ring gears. PT-2 could once again be rotated with no components contacting and the appropriate gear ratio.

PT-2 was then re-installed in the E-Drives Rig and more dynamic testing was performed. During initial testing, the mended modulator appeared to be holding up, but when testing was performed at higher speeds a noise indicating possible damage developed and testing was once again halted. Once removed from the test stand and partially disassembled, it was clear that the repaired pole piece and its supports were not able to withstand the forces exerted on them. The repaired pole piece was completely shredded. Single lamina layers were found in both inner and outer air gaps, with some shards piercing the carbon fiber hoop retaining the sun gear's magnets. The damage to the modulator can be seen in Figure 20 below with lamina still strewn about its surface. Due to the significant damage observed, the possibility of the structural integrity of the carbon fiber hoop bounding the sun gear being compromised, and the high cost associated with what was determined to be appropriate rebuild steps, it was decided to retire both the modulator and magnetic arrays of PT-2.

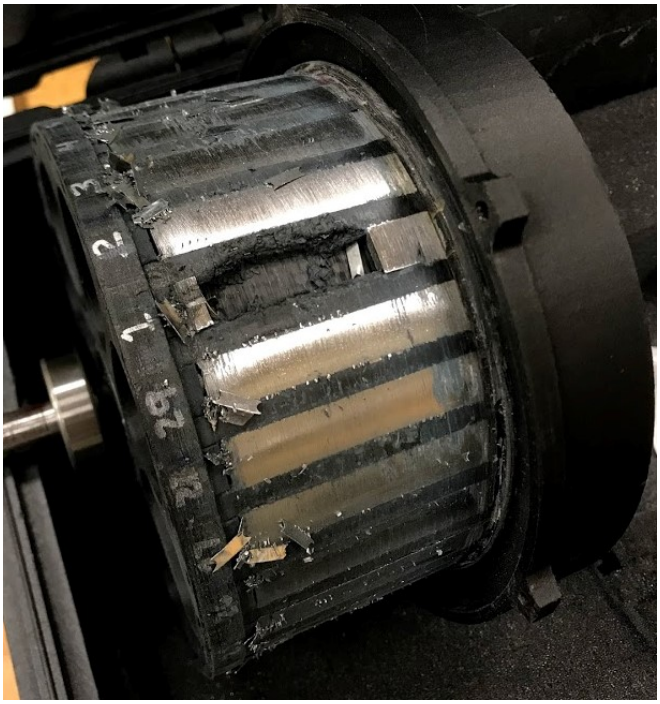

Fig. 20. PT-2 second modulator after being rebuilt and tested again with replacement pole piece and mended structural posts failing.

CONCLUSIONS

Lessons learned in the development and fabrication of PT-2 were numerous. Although operation and testing of PT-2 was limited, it offered a high-specific-torque (44 Nm/kg) and exhibited its expected gear ratio when dynamically tested. It also provided key insight into critical fabrication elements of high-specific-torque concentric magnetic gears. Specifically, it brought to attention the necessity for a structurally sound modulator. It has become clear through this body of work that in order for magnetic gears to be lightweight, the modulator and air gaps must be fairly thin. This drives a requirement for minimal deflection in the modulator when dynamically loaded. Stiffer pole pieces and support posts that can withstand the magnetic and centrifugal forces seen in operation will be an area of focus for the group moving forward. Structural materials with high stiffness, high strength, negligible magnetic interference, high electrical resistivity (to minimize eddy current losses), and high thermal conductivity (to remove waste heat) are being explored. Incorporation of such materials will be critical to improvement of CMG's specific torque and efficiency, enabling their introduction to aerospace propulsion systems.

Moving forward, the project is continuing work on manufacturing and assembly of PT-3, a high efficiency magnetic gear, PT-4, a magnetic gear designed for NASA's quadrotor concept vehicle (Refs. 18, 19), and a magnetic gear prototype sized for the Maxwell X-57 high lift propulsors. Lessons learned in this body of work have been implemented in the fabrication of PT-3 to improve manufacturing and assembly and are already yielding promising results. Additional lessons from PT-3's build phase will inevitably be included in the fabrication of PT-4 and the X-57 prototype as well. Implementation of more effective fabrication methods will decrease the likelihood of air gaps closing, and components rubbing against one another. These improvements will boost performance, reliability, and durability of CMG's.

ACKNOWLEDGMENTS

This work was supported by NASA's Independent Research and Development (IRAD) Program and Revolutionary Vertical Lift Technology (RVLT) Project.

REFERENCES

[1] Asnani, V. M., Scheidler, J. J., and Tallerico, T. F., "Magnetic Gearing Research at NASA," American Helicopter Society 74th Annual Forum Proceedings, Phoenix, AZ, May 2018.

[2] Scheidler, J. J., Asnani, V. M., and Tallerico, T. F., "NASA's Magnetic Gearing Research for Electrified Aircraft Propulsion," 2018 AIAA/IEEE Electric Aircraft Technologies Symposium (EATS), National Harbor, MD, July 2018.

[3]Moore, M. D., "Misconceptions of electric aircraft and their emerging aviation markets," 52nd Aerospace Sciences Meeting, 2014.

[4]Nicola, F. D., Sorniotti, A., Holdstock, T., Viotto, F., and Bertolotto, S., "Optimization of a Multiple-Speed Transmission for Downsizing the Motor of a Fully Electric Vehicle," *SAE International Journal of Alternative Powertrains*, Vol. 1, (1), 2012, pp. 134–143.

[5]Arkkio, A., Jokinen, T., and Lantto, E., "Induction and permanent-magnet synchronous machines for high-speed applications," 2005 International Conference on Electrical Machines and Systems, Vol. 2, 2005.

[6]Rahman, M. A., Chiba, A., and Fukao, T., "Super high speed electrical machines-summary," IEEE Power Engineering Society General Meeting, 2004., 2004.

[7]Harris, F. D., Kasper, E. F., and Iseler, L. E., "US civil rotorcraft accidents, 1963 through 1997," Technical report, NATIONAL AERONAUTICS AND SPACE ADMINISTRATION MOFFETT FIELD CA AMES . . . , 2000.

[8]Liu, L. and Pines, D., "Analysis of US Civil Rotorcraft Accidents Caused by Vehicle Failure/Malfunctions, 1998 to Present," American Helicopter Society 61st Annual Forum, Grapevine, TX, 2005.

[9]Sheng, S., "Gearbox Typical Failure Modes, Detection, and Mitigation Methods (Presentation)," , 1 2014.

[10]Holden, J. and Goel, N., "Fast-forwarding to a future of on-demand urban air transportation," *San Francisco, CA*, 2016.

[11]Gerber, S. and Wang, R., "Analysis of the end-effects in magnetic gears and magnetically geared machines," 2014 International Conference on Electrical Machines (ICEM), Sep. 2014.
doi: 10.1109/ICELMACH.2014.6960211

[12]Li, X., Chau, K.-T., Cheng, M., and Hua, W., "Comparison of magnetic-geared permanent-magnet machines," *Progress In Electromagnetics Research*, Vol. 133, 01 2013, pp. 177–198.
doi: 10.2528/PIER12080808

[13]Jian, L. and Chau, K. T., "A Coaxial Magnetic Gear With Halbach Permanent-Magnet Arrays," *IEEE Transactions on Energy Conversion*, Vol. 25, (2), June 2010, pp. 319–328.
doi: 10.1109/TEC.2010.2046997

[14]C. Gardner, M., Johnson, M., and A. Toliyat, H., "Comparison of Surface Permanent Magnet Axial and Radial Flux Coaxial Magnetic Gears," *IEEE Transactions on Energy Conversion*, Vol. PP, 08 2018, pp. 1–1.
doi: 10.1109/TEC.2018.2865200

[15]Gerber, S. and Wang, R., "Evaluation of a prototype magnetic gear," 2013 IEEE International Conference on Industrial Technology (ICIT), Feb 2013.
doi: 10.1109/ICIT.2013.6505692

[16]Matthee, A., Gerber, S., and Wang, R.-J., "A high performance concentric magnetic gear," , 01 2015.
doi: 10.13140/RG.2.1.1493.6167

[17]Frank, N. W., *Analysis of the concentric planetary magnetic gear*, Ph.D. thesis, 2011.

[18]Silva, C., Johnson, W. R., Solis, E., Patterson, M. D., and Antcliff, K. R., "VTOL Urban Air Mobility Concept Vehicles for Technology Development," 2018 Aviation Technology, Integration, and Operations Conference, 2018.

[19]Johnson, W., Silva, C., and Solis, E., "Concept Vehicles for VTOL Air Taxi Operations," AHS International Technical Meeting on Aeromechanics Design for Transformative Vertical Flight, San Francisco, CA, 2018.